MONITORING AND MANAGEMENT OF WATER POLLUTION IN AN IMPROVISED LABORATORY

M.Sc. Dissertation under the supervision of Prof. Dinesh Mohan
10 June 2020
School of Environmental Sciences
Jawaharlal Nehru University, Delhi

Shairik Sengupta (Reg. 54356)

Contents

MONITORING AND MANAGEMENT OF WATER POLLUTION IN AN IMPROVISED LABORATORY

ABSTRACT

The present work concerns water quality testing during the period of Covid-19 lockdown in India, using either easily available electronics or constructing measurement devices, as the situation demanded. It also describes the development of a biochar for water purification and an assessment of its powers, all without any laboratory equipment. Measurements of filter efficiency were found to be so encouraging that the filtered water was used for synthesizing hand-sanitizer for free distribution during the Covid crisis.

INTRODUCTION

The environment surrounds everyone, but information about its quality sometimes can be as difficult to obtain as an unpolluted environment. This information is generated mostly in laboratories fitted with sophisticated equipment and disseminated in academic circles. However, knowledge that concerns everyone should not be restricted to laboratories. This necessity manifested especially strongly when a "Lockdown" was slapped on India on 25th March 2020 and environmental monitoring remained locked in the laboratories. The situation provided an opportunity to this researcher to improvise water quality monitoring and management solutions during April-June 2020.

Water quality can be assessed by various parameters. Color which can be seen with the naked eye is a general indicator,[1] but a spectroscopic analysis provides great insight into the properties of a solution, as interaction of a solution with different wavelengths of light electromagnetic radiation depends on the composition of the solution. Spectroscopy has traditionally been a domain of experts (the author has, in various points in his life, heard from a multitude of seniors that he cannot go near the spectrophotometer alone). Scheeline et al.[2] described the development of a simple camera-based spectrophotometer that would not only be good enough to teach the principles of spectrophotometry to American children, but also for detection of chemicals in laboratories in Vietnam. Nandiyanto et al.[3] in Indonesia developed their own version of a spectrometer, and used it extensively in their research. A lot of progress has been made in making inexpensive spectrophotometers, and establishing that they work well[4,5,6,7,8,9]. Fonseca et al.[10,11] reported the construction and evaluation of LED based spectrophotometers. Some have used CDs to diffract light[12], others have used cameras to analyze intensity of various wavelengths[13]. The Fe^{3+} and Fe^{2+} content in several river waters were analyzed using an LED by Yasutada[14]. Murray et al.[15] took this a step further, into the UV region and worked on NO_3^- and NO_2^- estimation. The NIR region has also been used as a fingerprint[16,17] for comparing the spectral profile of various water samples. Hussain et al.[18] have demonstrated the applicability of these instruments in India. Prairie et al.[19] formed an international team and tested out their version of a LED spectrophotometer in various waters of the world. Various species of substances like (Hg^{2+}),[20] (Cr^{6+}),[21] (K^+),[22] (Cl^-) and (NO_3^-),[23] (Fe^{3+} and Fe^{2+}),[24] (F^-),[25] (PO_4^{3-})[26] have been successfully detected and quantified using these instruments. Recent developments understandably focus on using smartphones[27,28].

The present work uses a Spectrophotometer cum turbidity meter built using an RGB and Amber LED as a light source, and a Photoresistor as the receiver, coupled to a multimeter to measure the resistance which decreases inversely with incident light intensity. Along with this, a Sparkfun Spectral Triad sensor[29] (used with impressive results in Hobbs' work on Mars Rover development[30,31]) coupled to an Arduino UNO[32,33] is also used to capture the reflectance spectra of water samples. These instruments are driven by open source software[34,35], so, the monitoring scheme described in this work can be replicated by anyone who wishes to do so. The sensors developed here can easily be adapted to work in sensor networks as explored in Malawi,[36] India,[37,38] China,[39] Australia,[40] and various parts of the world.[41,42] This approach requires the components to be inexpensive yet reliable.

Measurement leads to a more anthropocentric problem: water may be polluted, and just knowing how polluted it is does not alleviate anyone's problems, unless it can be treated too. A very popular tool for this is biochar. Biochar is an ancient idea originating in the Amazon.[43] Biochars can be made from pyrolyzing a host of biogenic materials, ranging from human manure,[44] through plastic wastes,[45] to agricultural byproducts[46] and wastes[47]. Various biochars have been characterized extensively,[48,49] their effectiveness as a sorbent for water treatment has been explored in depth.[50] They can be used to remove color,[51] various metal ions,[52] anions,[53] and organics.[54] Their modifications like magnetization[55] also form a major part of current research in the field.

However, for real life applications, easy manufacturability of an effective biochar is essential, and performance of char synthesized in laboratory conditions would not be applicable to local concoctions. Surprisingly, all work in this field describes chars developed in laboratories (except for some gardening enthusiasts on YouTube who have posted videos of lighting biomass on fire and mixing it with soil). Here, a char is synthesized in a kitchen, and its performance is evaluated using easily available electronics.

The biochars synthesis and its performance evaluation system described here is easily replicable, even by the layman. methods developed in this work are based on low cost electronics that are available everywhere. Easily available and dependable environmental monitoring and management pave the way for citizen participation,[56] which can result in major improvements.[57]

MATERIALS AND METHODS

To analyze the spectral characteristics, a spectrophotometer cum turbidity meter was built (in the author's home in Kolkata) as described next (Figure 1). The light sources are two LEDs, one RGB and one amber. An Arduino UNO was used to control the color (only the red, green and blue colors are used, as the led cannot produce any other frequency), a laptop always plugged to a wall outlet was used as a power source to maintain a stable current to avoid light intensity fluctuations. Light intensity was measured with a photoresistor. Only one color was used at a time, as photoresistors are not tuned to any particular wavelength. Their sensitivity varies across the spectrum, but this variation is accounted for in this report, as a color-specific scale is adopted for comparisons. Some error is expected to come from wavelength changes from light-particle interactions. Measurement of light intensity at 0° gives the Absorbance/ transmittance, measurements at 35°, 90°, and 135° gives the scatter. From these values a scatter profile is determined to draw inferences about particle sizes in solution. Scattering thus measured is also used to determine turbidity.

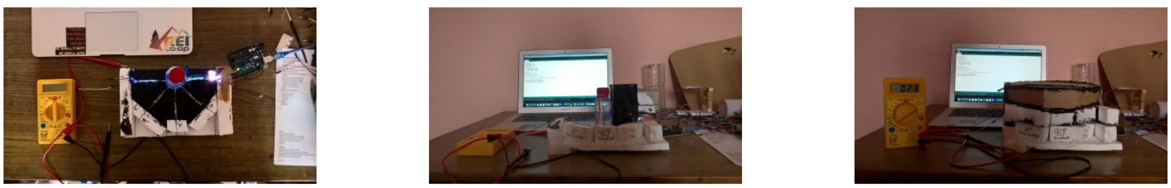

(a) (b) (c)

Figure 1: Spectrophotometer-cum-turbidity meter: (a) Top view, configuration (b) Side view, configuration
(c) Working condition with black painted polystyrene shroud to block external light

A Sparkfun Spectral Triad sensor (AS7265x) driven by an Arduino UNO was used to obtain reflection spectra of samples (Figure 2). These spectra are compared to draw conclusions about water quality.

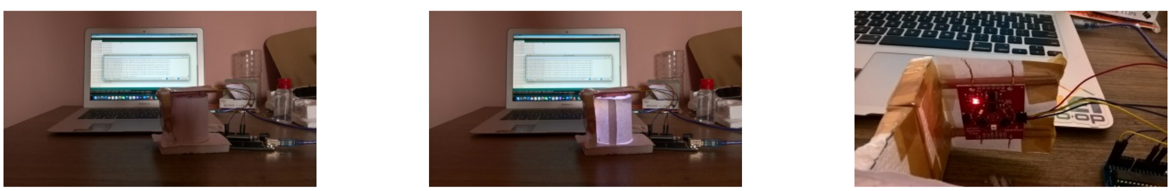

(a) (b) (c)

Figure 2: The spectral triad: (a) Set-up (b) Working conditions (c) The sensor

A pH meter also based on Arduino (DFrobot SEN0161) was used to measure the pH of all samples, after calibration against standard buffers. (Figure 3)

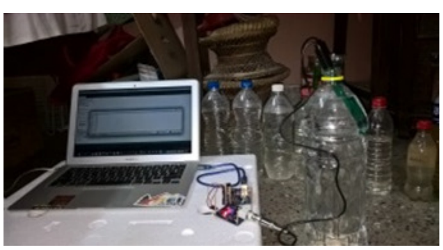

Figure 3: PH meter set-up

All experiments were conducted at 25°c, as the work of Sukmafitri et al.[58] indicated errors are lesser at lower temperature for similar sensors.

To check the performance of the spectrophotometer and the Spectral Triad, solutions of various concentrations were prepared by serial dilution for red, yellow, blue and green watercolor (pigment composition could not be obtained from the manufacturer, but this is inconsequential, as the ultimate goal here is to check the performance of the instruments, not to detect or quantify presence of watercolors in water). The serial dilution technique offers the great advantage that as long as the solute can be quantified accurately once, we can keep measuring the solution for the rest of the procedure without introducing significant error. Small quantities are difficult to measure without sophisticated equipment, so the entire volume of paint (3ml) was dissolved in an accurately graduated 600 ml cylinder (5000ppm), and further dilutions were produced in sufficiently large quantities to avoid error. The water color set used in this experiment cost 20 rupees, for 12 colors.

The water samples were collected from various *ghats* (Figure 4) of the river *Hooghly* in Kolkata on 8th May, towards the end of the lockdown. The locations were *Ahiritola Ghat*, *Jagannath Ghat*, *Babughat* and *Princep Ghat*. People living in *ghats* were extremely cooperative, and showed the author the way around various locked gates.

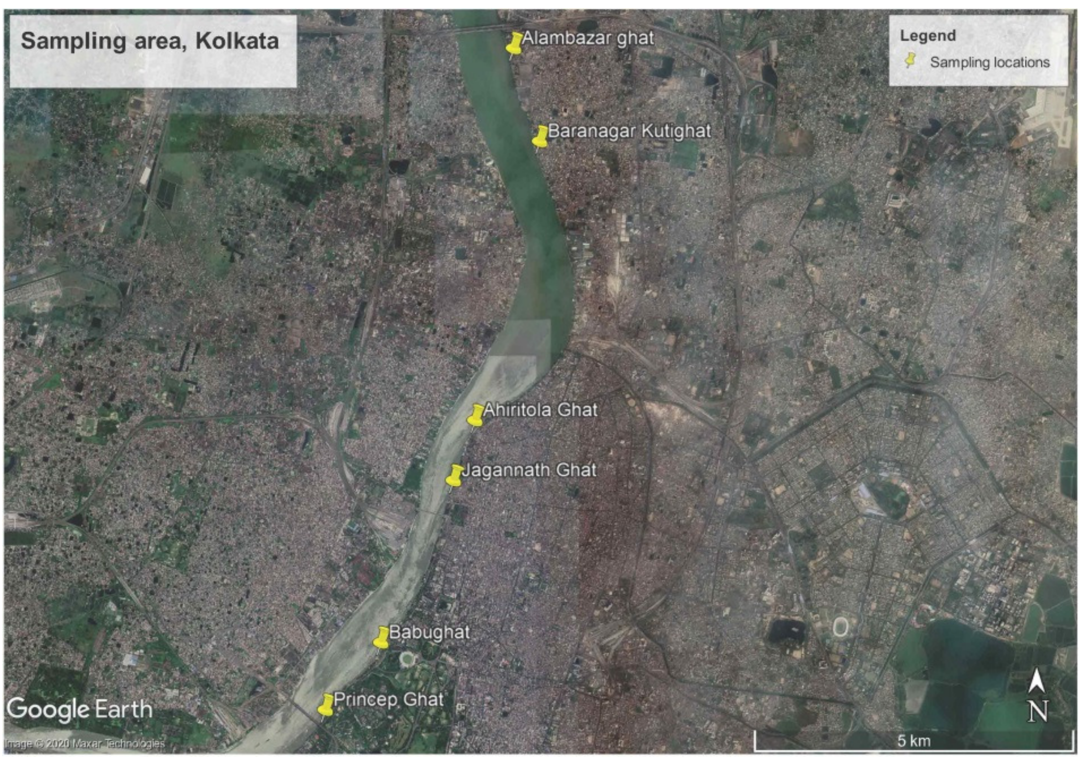

Figure 4: Sampling locations

Water was also collected post lockdown, on 5th June, from *Alambazar Ghat*. Another Sample was taken one day after cyclone *Amphan* ravaged Kolkata. This sample was taken from

Baranagar Kutighat on 20th June. All samples were taken during the ebb, so the upstream and downstream descriptions of direction are valid.

To prepare biochar, sugarcane bagasse was collected from a street-side sugarcane juice seller (Figure 5). The reason for selecting bagasse is twofold – they are known to be effective for removing both organics[59] and inorganics such as chromium,[60] Arsenic,[61] Cadmium and Zinc,[62] and they are freely available. All of these are known to be in concentrations of concern in Ganges water.[63,64,65,66,67]

Figure 5: Street-side sugarcane juice seller, from whom bagasse was collected

Figure 6: Filtering set-up

The bagasse was heated for various time periods, in a closed vessel, on a gas stove. The gas burner was calculated to have a power of 656.3 watts (from time required to boil water from room temperature). Temperature achieved by the biomass cannot be calculated easily,[68] and there was no adequate thermometer that could be stuck inside the vessel. Therefore, no attempt is made in this work to report the production temperature of the chars. While chars produced in this way cannot have an oxygen free environment, most of the oxygen present in the vessel is used up in turning the outer layers of the biomass to ash. This leaves the rest of the biomass with the low oxygen environment required for char formation. Another important consideration is that some little vent needs to be kept in the configuration, to let VOCs escape (can be seen as a brownish smoke during production, which condenses into a black goo on the sides of the vessel). The fact that air is indeed forced to escape the vessel and leaves an oxygen deprived environment behind is reflected in the fact that once the burner is turned off and the vessel covered securely, leaving no vents, after some time it takes some effort to pull off the lid.

Six chars were prepared: by heating biomass for 10, 20, 30, 40, 50 and 60 minutes. The 60-minutes char has been dropped from subsequent analysis as the vessel had been stuffed by huge pieces for preparing that char, which resulted in a disaster: some pieces were left totally uncharred. It did however teach one valuable lesson: best results are obtained when the bagasse is torn up in small pieces.

The char obtained was stuffed in cut up plastic bottles to construct filters. 5 g char was put as filter in each bottle, 1 liter of polluted water was passed. Water taken from the *Hooghly* (post lockdown) was filtered.

All electronics were purchased from Robu.in,[69] all sampling was done on a cycle to avoid unnecessary attention from enforcers who severely violate social distancing to implement lockdown.

RESULTS AND DISCUSSION

PERFORMANCE OF THE TURBIDITY METER

The performance of the spectrophotometer needs to be checked. To do this, a series of solutions of various concentrations were prepared, for the red, yellow, green and blue dyes. These four colors were selected as these correspond to the colors of the four LEDs used in the set-up, and linearity of absorbance with concentration needs to be checked for all the wavelengths the instrument works in. Absorbance (measurements at 0° point in the turbidity-meter set-up) and concentration relationships are shown in the charts below (Table 1). The log scale used in the horizontal axis of Table 1 is required to capture the entire range of concentrations used for verification of the instrument's capabilities.

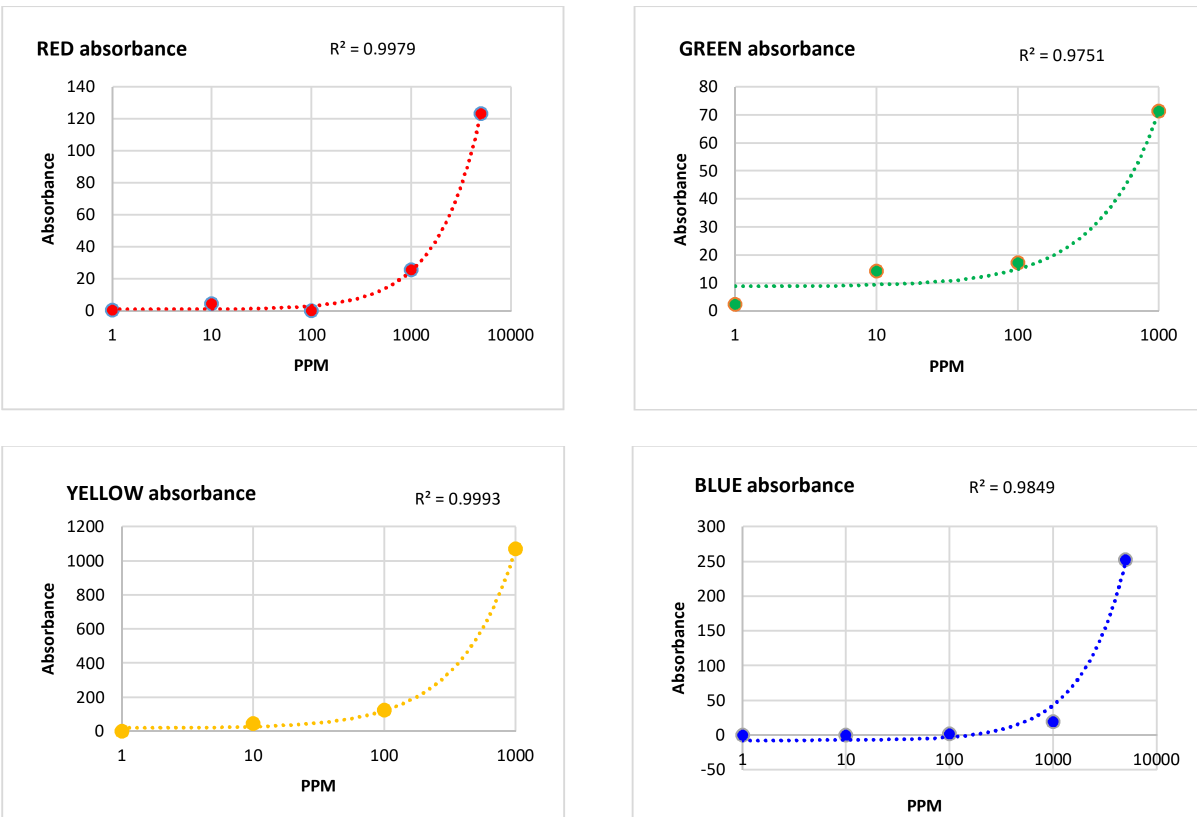

Chart 1

Not only does the instrument show great sensitivity, it does so over a remarkable range of concentrations. The observations here testify that the instrument can indeed reflect the linear change of concentrations as a linear change in absorbance count. Count is an arbitrary unit in any spectrophotometer, in the present case the count is the resistance of the photoresistor. The lowest resistance is obtained for drinking water (more transparent for a given frequency of light than solutions of color corresponding to that frequency). As the concentration increases, lesser and lesser light reaches the photoresistor, and its resistance increases.

Scattering of light at various angles, as a function of concentration is examined next (Chart 2). The intensity at each angle (shown in horizontal axis) is reported as a percentage (shown in vertical axis) of the intensity at 0° (transmission signal). Only the intensity at 30°, 90° and 135° are reported, so that a relative scale can be adopted. Experimentally this offers the advantage that a turbidity standard is not required. This representation offers a great tool for visualization: solutions of low concentration are of low turbidity, light intensity at all angles are close to the transmission signal intensity, resulting in a slightly convex curve; as turbidity increases, the curve turns more convex, reaching a transition point where it appears linear; this is followed by concave curves, where the solution is so turbid that incident light is scattered more than it is transmitted (the greater than 100% values in chart 2). Apart from this, higher values on the vertical axis can simply be interpreted as higher light intensity at a scattering angle. The yellow LED is not used in this section as its intensity is low to begin with. The Yellow signal can only be picked up at 35° at high concentrations, and at 90°, and 135° at concentrations high enough for the transmission signal to disappear below detectable limits.

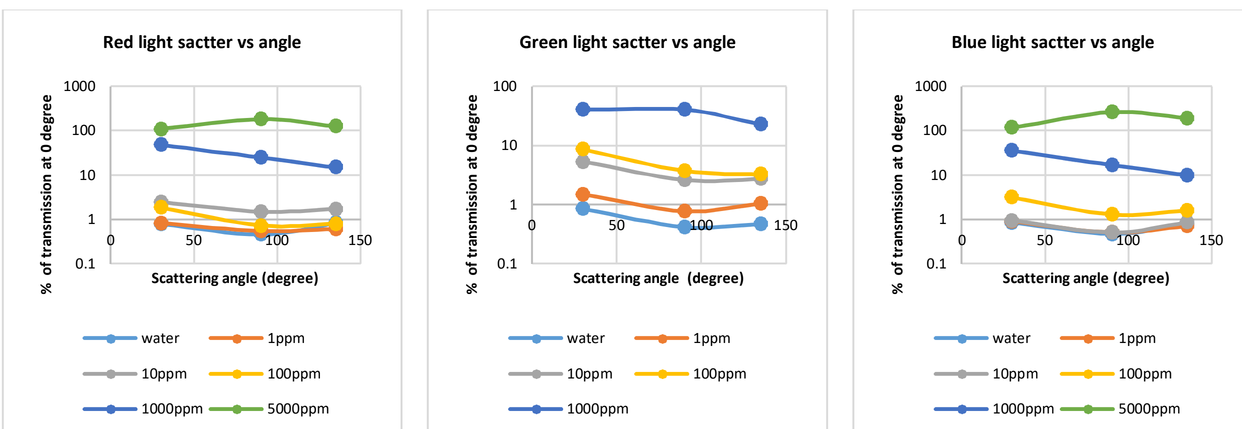

Chart 2

For all frequencies we see that the scattering increases at all angles. At extremely high concentrations, the 90°, and 135° signal dominates, as the solution becomes almost opaque.

Next the light intensities at each angle, as a function of concentration were considered, shown in the charts below (Chart 3,4 and 5).

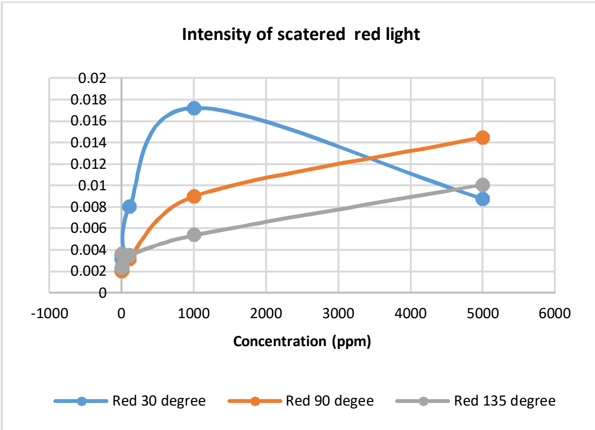

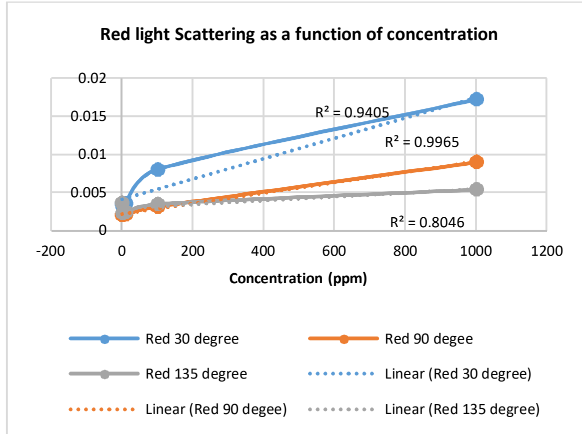

Chart 3

Chart 3 establishes that with respect to red light, the scattering is proportional to concentration of solution (and therefore turbidity).

Next we consider scattering of green light, and present similar charts.

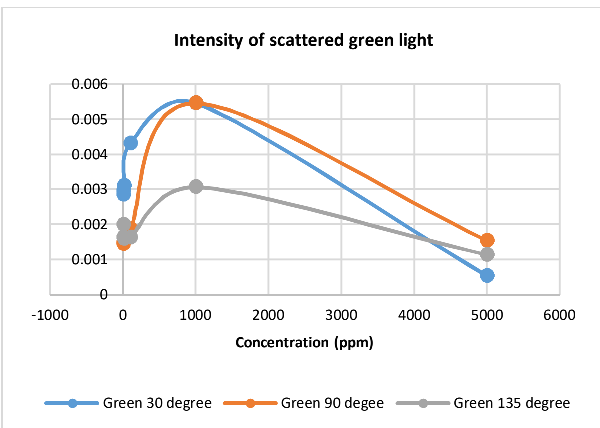

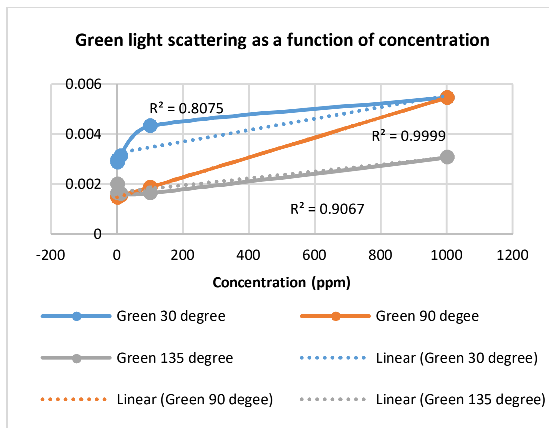

Chart 4

This proves that green light is also scattered proportionally to turbidity and concentration.

Finally, turning to blue light, we obtain similar results.

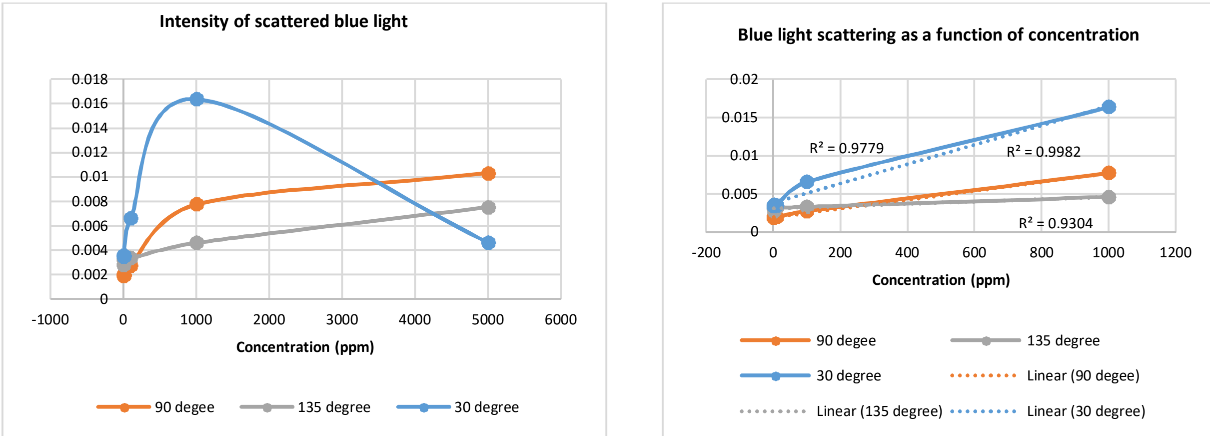

Chart 5

The above figures imply that blue light scattering is also proportional to concentration (and turbidity).

Similar tests were done for yellow light (chart 6). Unfortunately, using the present set up, scatter data is unobtainable for solutions that are not of extremely high concentration with the yellow light, as the transmission signal drops below detectable limits.

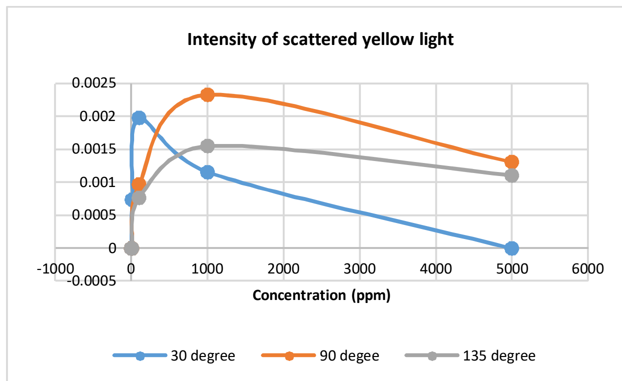

Chart 6

We can conclude from the curves presented above, that the instrument prepared is adept at measuring scattering, as a linear function of concentration and turbidity, and that the scattering at 90° is the best measure of turbidity, for all wavelengths.

ASESSING THE REFLECTION SPECTRA SENSOR (SPECTRAL TRIAD)

The reflection spectra of the red, yellow, green and blue solutions were recorded, in the red, yellow, green and blue regions respectively.

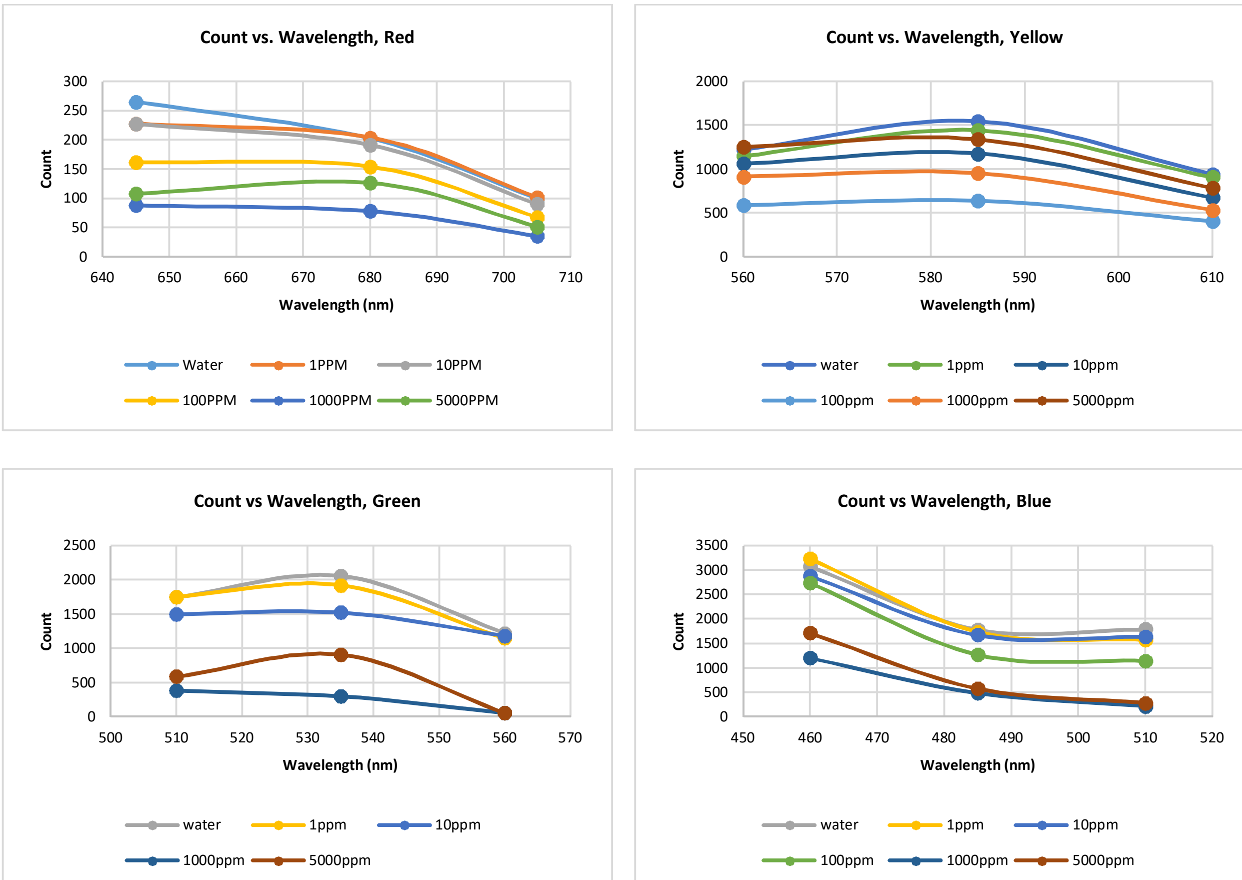

Chart 7

All the spectra look counter intuitive. Reflection count appears to be higher for pure water, and goes down for solutions of higher concentrations. This apparent paradox bewildered the author until realization hit, the Spectral Triad was meant to measure reflections of solid objects. The strategy of using it to take spectra of liquids results in some light traveling all the way through the solution and being reflected from the bottom of the cell, which essentially behaves as a virtual light source. The signal picked up by the sensor is predominantly this, a signal that is attenuated by travelling through the solution twice. The color we see is of a solution we see is the wavelength it most effectively reflects and scatters. Thus, a better insight into concentration can be achieved by taking reciprocal of the count. The explanation is further justified by the fact that the reflection count at the sensor actually starts increasing with concentration at extremely high concentrations, when the solution behaves almost as if it were opaque. Plots of wavelength vs this transformed count (reciprocal of the reflection count) for various concentrations are presented next, along with plots of transformed count at the inflexion point as a function of concentration (Chart 8).

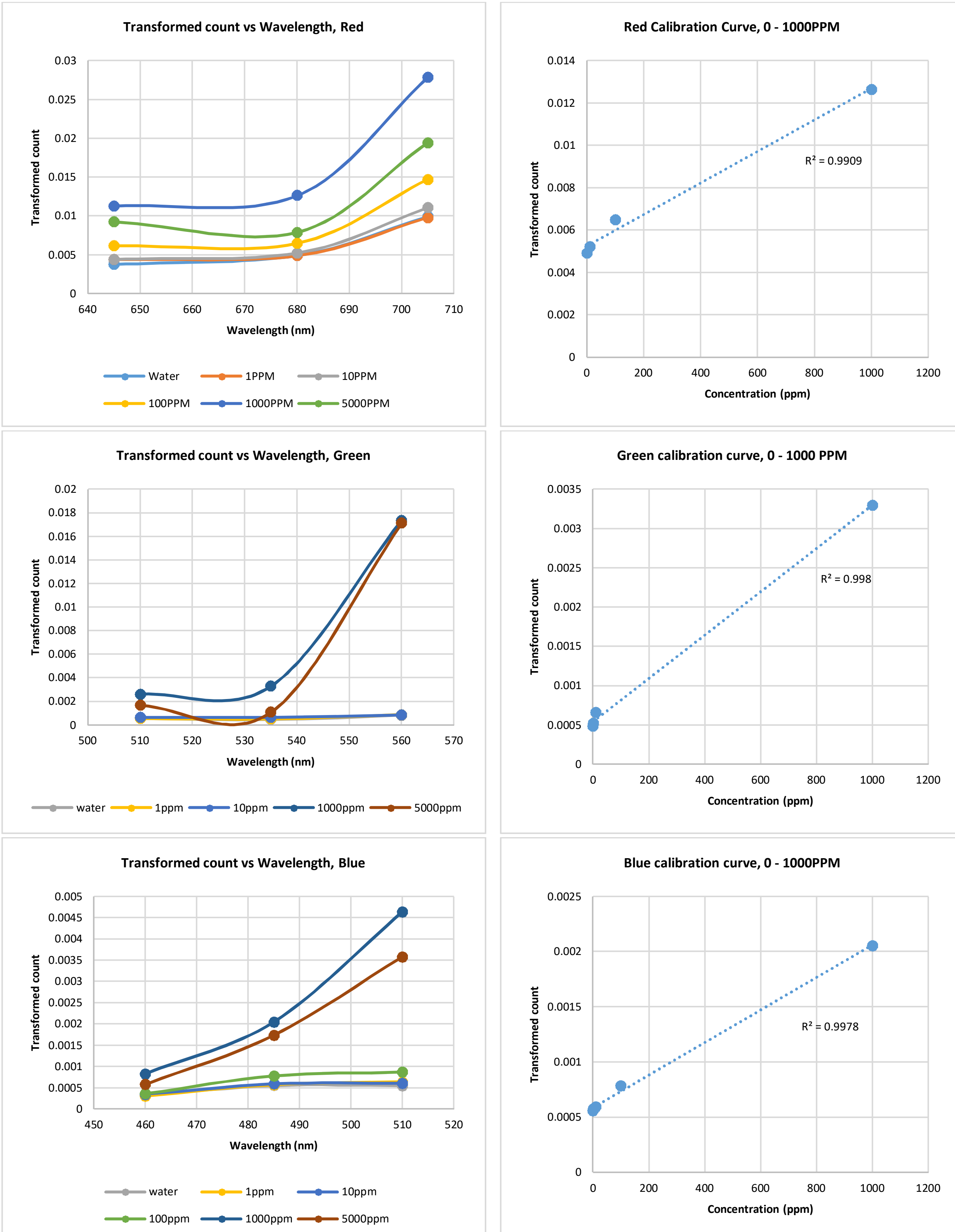
Transformed count vs Wavelength, Red
Transformed count
0.03
0.025
0.02
0.015
0.01
0.005
0
640 650 660 670 680 690 700 710
Wavelength (nm)
Water
1PPM
10PPM
100PPM
1000PPM
5000PPM
Red Calibration Curve, 0 - 1000PPM
Transformed count
0.014
0.012
0.01
0.008
0.006
0.004
0.002
0
0 200 400 600 800 1000 1200
Concentration (ppm)
R² = 0.9909
Transformed count vs Wavelength, Green
Transformed count
0.02
0.018
0.016
0.014
0.012
0.01
0.008
0.006
0.004
0.002
0
500 510 520 530 540 550 560 570
Wavelength (nm)
water
1ppm
10ppm
1000ppm
5000ppm
Green calibration curve, 0 - 1000 PPM
Transformed count
0.0035
0.003
0.0025
0.002
0.0015
0.001
0.0005
0
0 200 400 600 800 1000 1200
Concentration (ppm)
R² = 0.998
Transformed count vs Wavelength, Blue
Transformed count
0.005
0.0045
0.004
0.0035
0.003
0.0025
0.002
0.0015
0.001
0.0005
0
450 460 470 480 490 500 510 520
Wavelength (nm)
water
1ppm
10ppm
100ppm
1000ppm
5000ppm
Blue calibration curve, 0 - 1000PPM
Transformed count
0.0025
0.002
0.0015
0.001
0.0005
0
0 200 400 600 800 1000 1200
Concentration (ppm)
R² = 0.9978

Chart 8

As it turned out, the yellow solution turned opaque at lower concentrations than the other colors. Two Calibration curves could be obtained, one for the translucent, and one for the reflecting regime of concentration (Chart 9).

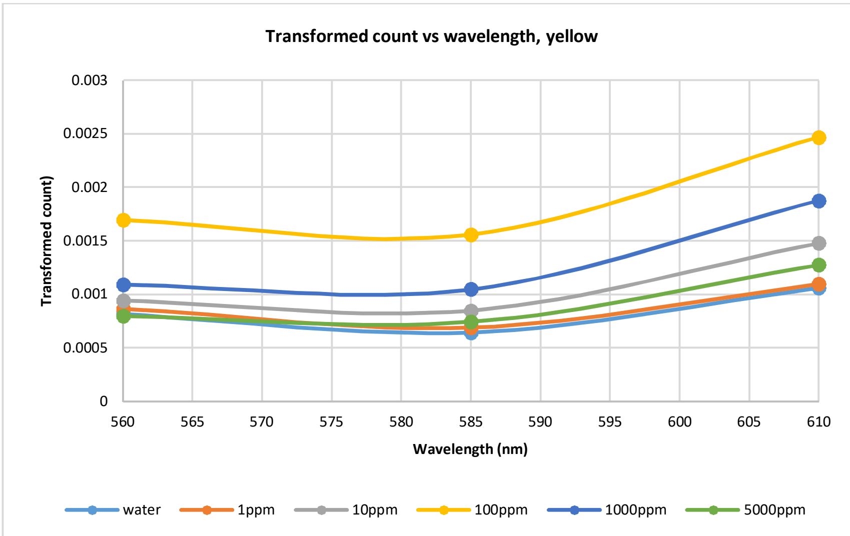

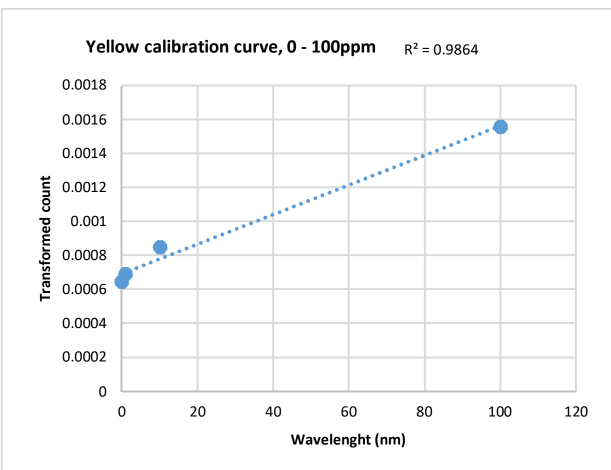

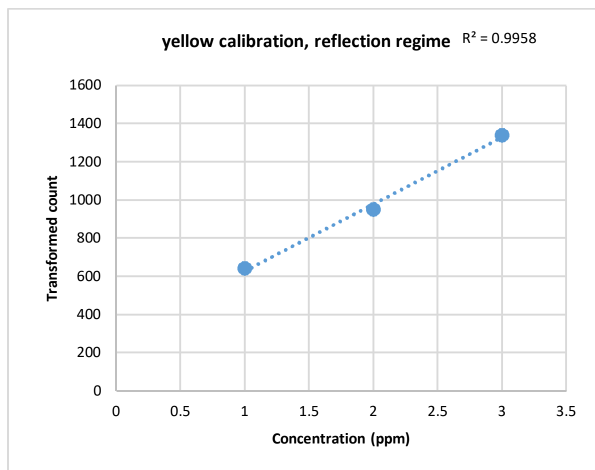

Chart 9

It transpires that the Spectral Triad can be used to acquire dependable data. The results obtained can be interpreted not only qualitatively (studying the similarities between spectral signatures), but also quantitatively (as a tool for estimation of concentration when the absorbance properties of a material are known). When comparing reflection spectra without transformations (as is done in this work, it should be kept in mind that a higher count indicates more clear water).

Samples of river water were obtained from four Ghats: Ahritola, Jagannathghat, Babughat, Princep Ghat.

The pH values of the samples of *Hooghly* water are given in Table 1. The water turns out to be basic (for natural water), but the pH reduces as one moves (South) towards the center of the city of Kolkata.

Typical *Hooghly* water	7.69
Ahritola Ghat	7.45
Jagannath Ghat	7.58
Babughat	7.36
Princep Ghat	7.07

Table 1

The scatter characteristics of the samples are given below (chart 10).

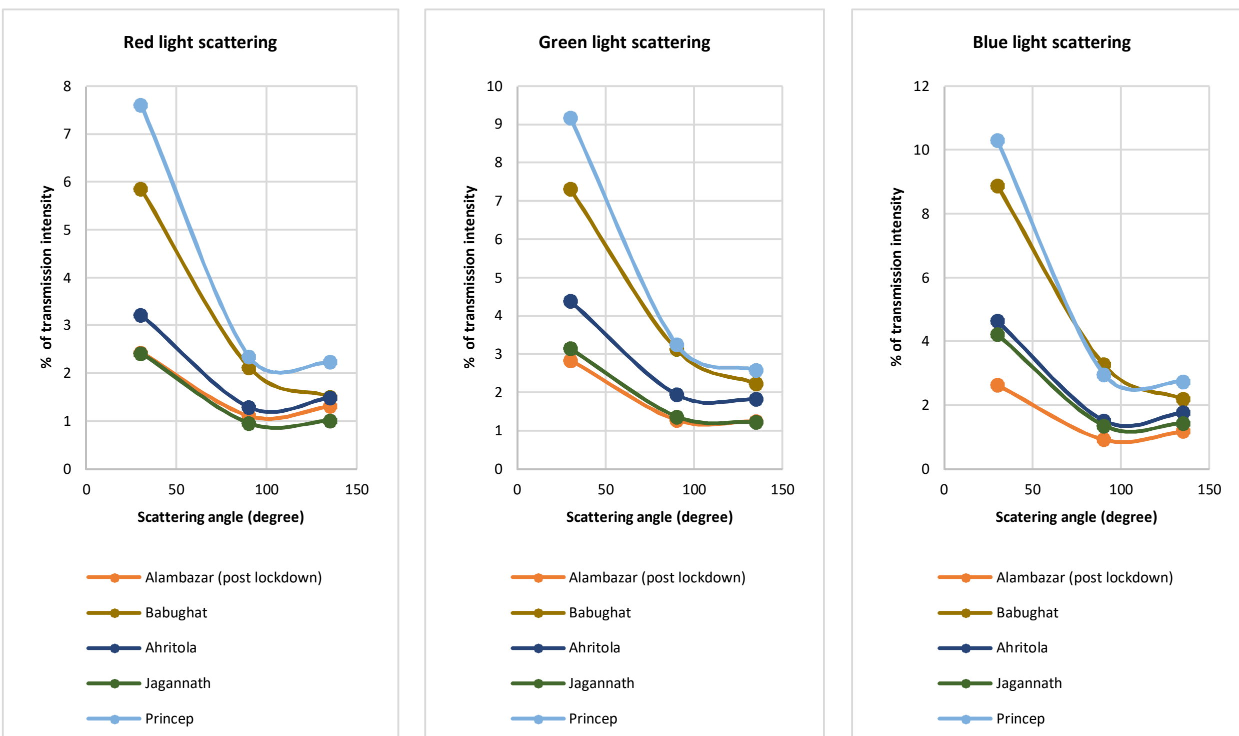

Chart 10: Scatter chractersistics of the samples across the spectrum

As the scattering profile is independent of wavelength, we can say the particles are approximately 1/4th the size of the red blue and wavelengths emitted by the LED. The larger front scatter signal indicates the presence of larger particles in the downstream sampling points, which is expected due to addition of waste water from the city's drains.

The higher turbidity values at 90° indicate the lockdown did not magically improve water quality, at least in terms of turbidity. This might be because a lot of people were staying in the ghats and their actions increased the turbidity.

Reflection spectra signatures are compared below.

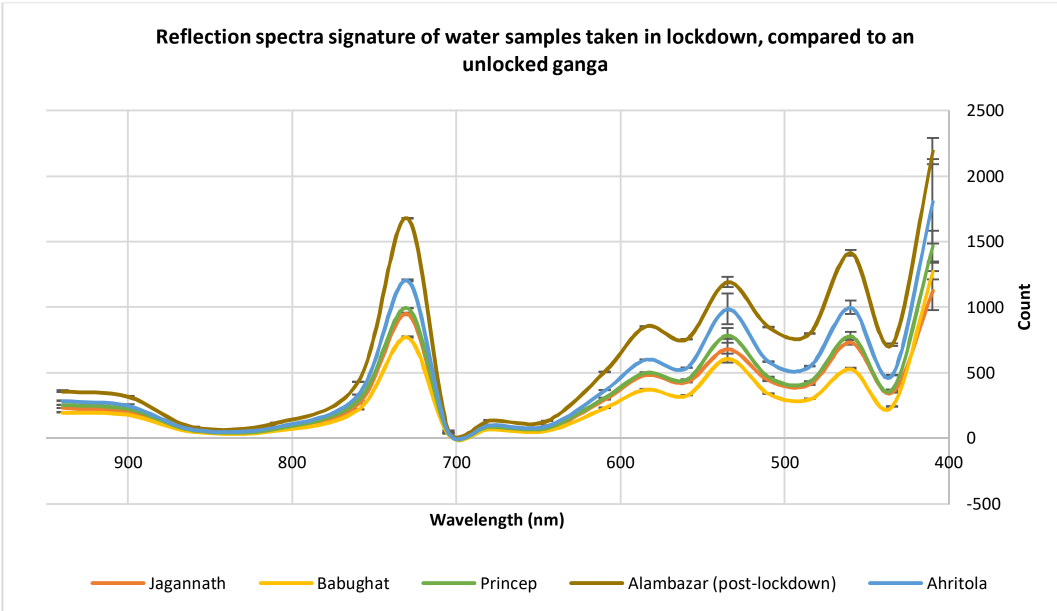

Chart 11: Reflection spectra of samples compared with post-lockdown water

The reflection spectra (Chart 11) confirm the previous finding. No major shifts for any chemical is seen.

The water sample collected from *Alamabazar Ghat* on 5th June 2020 is regarded as *typical Ganges* (*Hooghly*) *water* for the purpose of the present study. The accompanying picture shows the, and the results at different degrees of filtration. The sample on the far left is without filtration, and the other samples from left to right are arranged in increasing degrees of heat used in producing the char for filtering.

Figure7: Water sample, before and after treatment by different chars

The effect of filtration can be perceived visually. The chemical characteristics are given below.

Measurements of PH are presented in tables 2, 3, and 4.

Sample	PH
Typical *Hooghly*	7.69
10 min filtrate	7.41
20 min filtrate	7.74
30 min filtrate	7.75
40 min filtrate	7.76
50 min filtrate	7.71

Table 2

Sample	PH
Amphan	7.69
Amphan filtrate	7.74

Table 3

Sample	PH
Drinking water	7.29

Table 4

All the experiments regarding water treatment have been done in the PH of the water sample being treated.

Performance of char in removing turbidity is documented in chart 12. Turbidity is represented in the fashion described previously

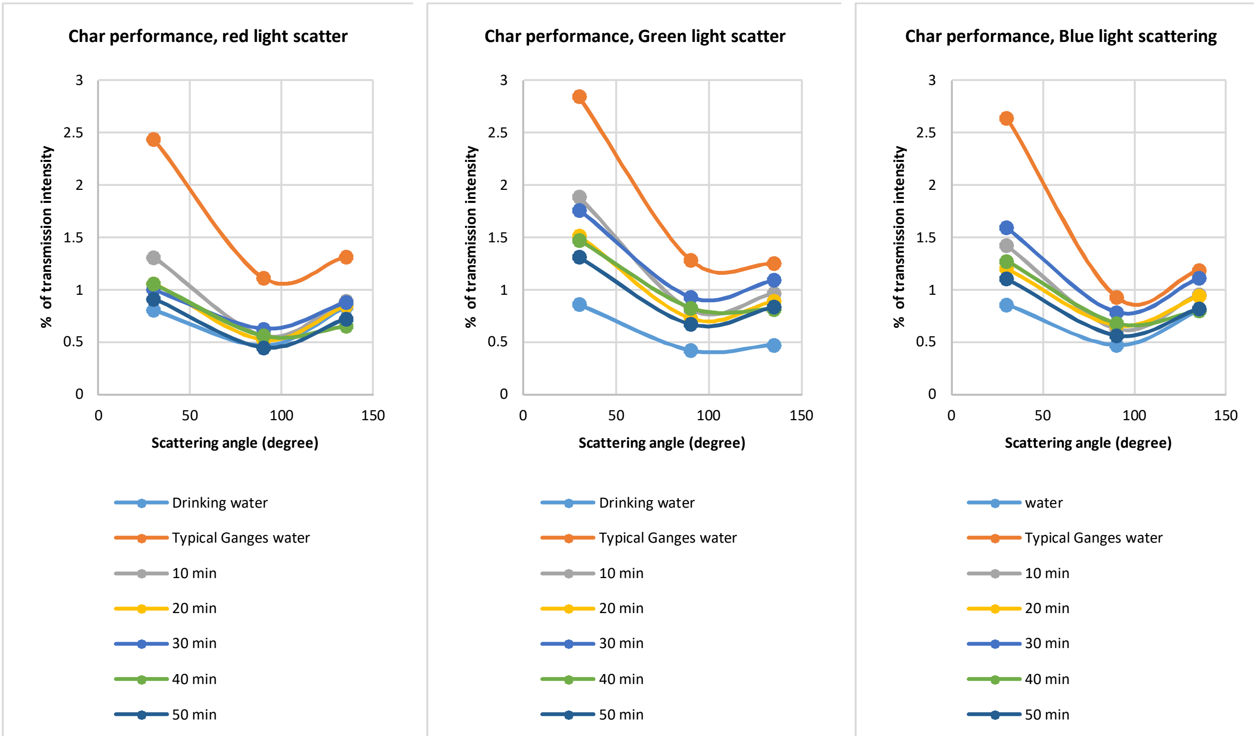

Chart 12

It can be seen clearly (chart 12) that the char produced by heating bagasse for 50 minutes in a closed vessel performs very well in removing turbidity from river water (scatter profile resembles that of water most closely).

Various materials present in water determine its absorption characteristics. The performance of the char in removing color producing material from water is presented in chart 13

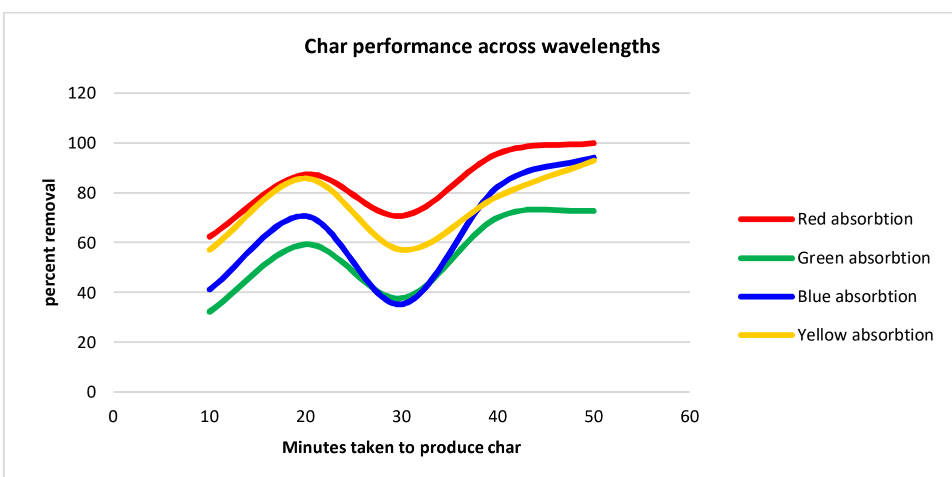

Chart 13: percent removal of transmission signal of various wavelengths, as a function of heat supplied during char production

The reflection spectra of the precursor *Hooghly* water, filtrates of the chars, and drinking water are presented below.

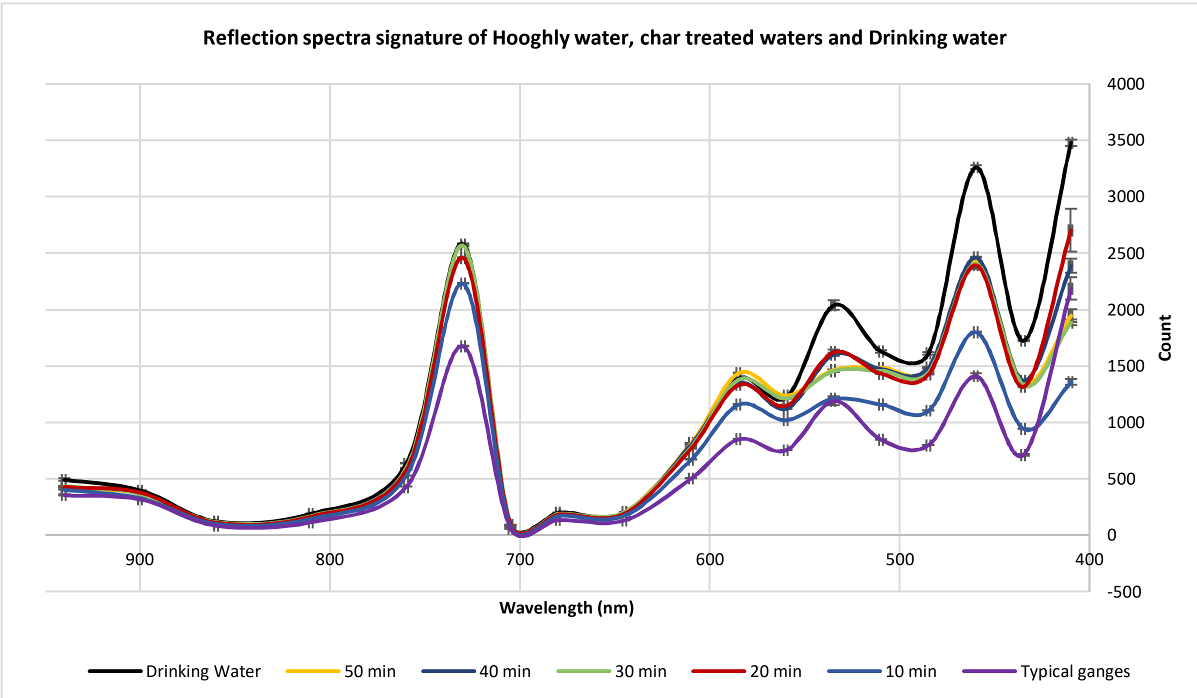

Chart 14: reflection spectra of polluted water and treated samples

By comparing the reflection spectra signatures, it appears that the char produced by pyrolyzing sugarcane bagasse by heating for 50 minutes performs the best. The performance parameters for char produced by supplying heat to sugarcane bagasse for 50 minutes in a closed vessel are summed up in table 5.

	Turbidity removal (at 90°)	Absorbance removal
Red region	102.994%	100%
Yellow region	Could not be calculated	92.857%
Green region	70.9113%	72.973%
Blue region	80.475%	94.118%

Table 5

A plot of percent removal of absorbance at each wavelength, as a function of heat supplied (expressed in minutes of heating) indicates the same (Chart 15).

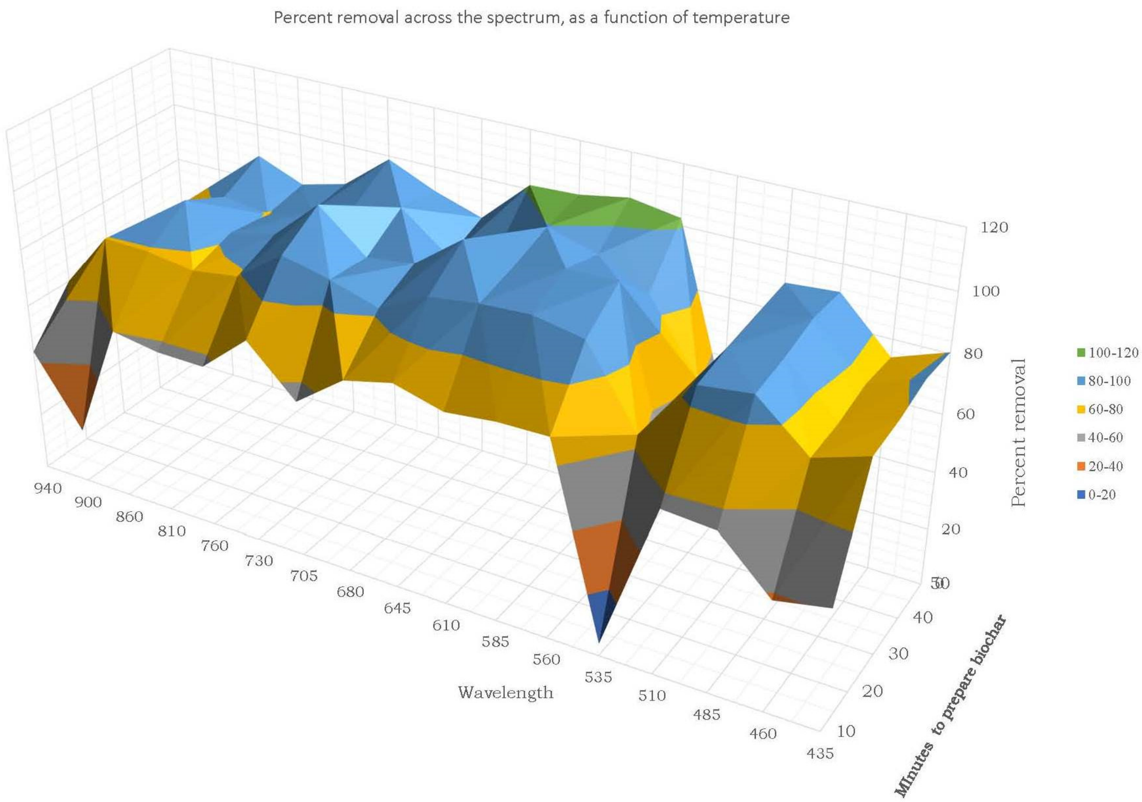

Chart 15: percent removal of absorbance at each wavelength as a function of heat supplied

As can be seen, the highest removal, over the broadest range of wavelengths is achieved by the 50-minute char.

We have now determined that the char produced at 50 minutes of heating performs best as a water filter.

At the time this work was being carried out, the cyclone *Amphan* arrived in Kolkata. The river water mixed with water logged drains and flooded conditions of the city. This water was put through the char as an acid test of is capabilities. A picture of the turbid water collected from *Baranagar Kutighat* and its filtered version is presented figure 8.

Figure 8: *Amphan* ravaged water: before and after treatment

The scattering characteristics of the pre- and post-flitration *Amphan* water are shown below (Chart 16), together with those of drinking water sample and typical Ganges water sample for reference.

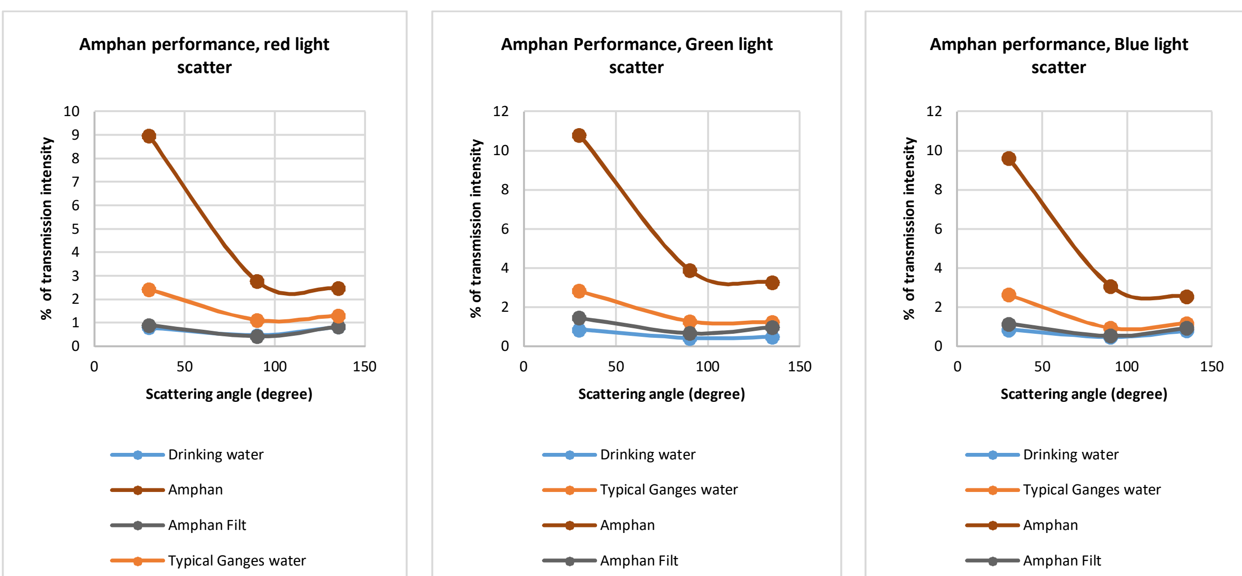

Chart 16

Clearly, the appalling scatter characteristics of the post *Amphan* river water have improved substantially after treatment.

The reflection signatures also reflect this (Chart 17).

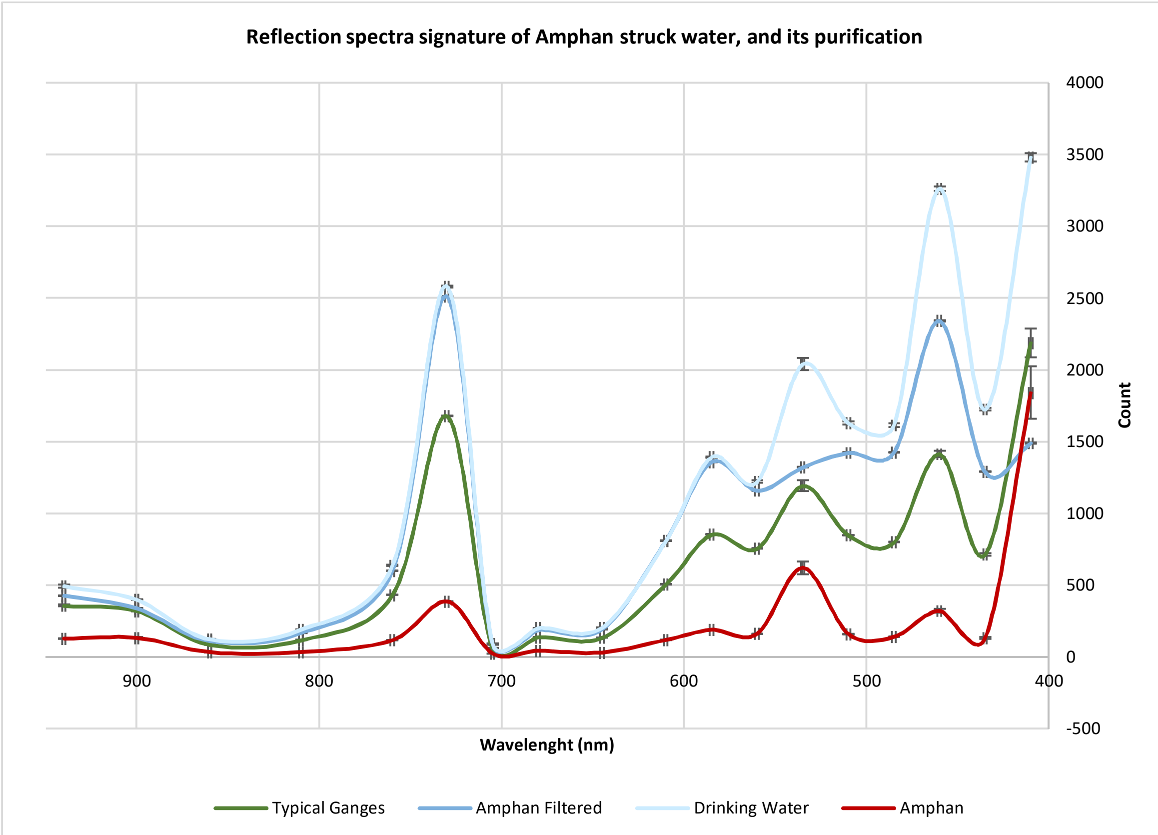

Chart 17

It may be noted that the impressive results shown here are obtained after passing the *Amphan* struck water through the filter just once.

CONCLUSIONS

The Spectral Triad can be used reliably to generate reflection spectra, the comparison of which can serve as a metric of purity/ pollution levels. The low cost and easy operability of the instrument can be exploited for application in remote areas. It also offers an advantage over conventional spectrophotometry, as a cuvette is not required for its operation, opening up possibilities for real time water quality monitoring.

The spectrophotometer cum turbidity meter developed here is arguably the world's cheapest version of the instrument (19 rupees for the LEDs, 400 rupees for the multi-meter, 425 rupees for the Arduino board). Though the instrument described here costs 844 rupees (excluding paint, gum and a polystyrene sheet), the price tag can be lowered even more if the Arduino is made to measure resistance directly (or the Arduino is dropped altogether, and LEDs are operated manually with batteries).

The scattering tests of river water quality during the Covid-19 lockdown show that the water quality was comparable to normal conditions upstream from Kolkata. The slightly higher values are likely due to an increased number of people living near the river. The effects of discharges from Kolkata on increasing the *Hooghly* River's turbidity can also be seen; there are some things the lockdown could not cure.

The reflection spectra display similar trends, and also display that no major chemical change took place due to the lockdown.

The char produced in a kitchen after 40 to 50 minutes of heat supply is found to perform exceptionally well, in PHs of natural conditions. (for a comparison, check appendix for an orthodox analysis of performance of a conventionally produced energy cane biochar in removing Congo Red dye: this char could remove the dye well only at extremely low PHs). The present work paves the way for further analysis on determining the applicability and limitations of biochar produced in natural settings. The experiments conducted here also validate the production process and offer a template for anyone in need of producing a low cost water filter.

Figure 9: The biochar filter in action, helping fight COVID-19 by purifying water for sanitizer synthesis

When the Covid-19 lockdown started, hand sanitizers became the most sought after and the least available item on the market. Where it was available, it was being sold for at least twice the normal price. Biochar produced in the fashion described here was used to filter water for synthesizing sanitizers at less than half the usual market price (apparatus shown in accompanying picture). More than 3000 bottles of sanitizer were distributed for free among people who needed it, driven by a crowdfunding campaign.

The char described also performed well in filtering polluted water after Kolkata's encounter with cyclone *Amphan*. The good performance of the char in this scenario opens up possibilities for use of biochar synthesized by citizens, especially in emergencies, and quite viably in everyday life.

ACKNOWLEDGEMENTS

I would like to thank my supervisor Prof. Dinesh Mohan for his guidance and patience. My lab mates also deserve applause for all their help. A special word of thanks to my friends and especially Megha who by now has reached a point of not telling me something can't be done, and just watching me with silent amusement. Saumya made classes more interesting. Of course, this acknowledgement would be incomplete without an expression of gratitude towards the entire JNU community. We learnt in the best possible way, that knowledge cannot be a closely guarded secret, access to it should be open for all.

BIBLIOGRAPHY

[1] Clair N Sawyer, Perry L. McCarty, Gene F. Parkin (2003). *Chemistry for Environmental Engineering and Science*, McGraw-Hill series in civil and environmental engineering, McGraw-Hill Education.

[2] Alexander Scheeline (2010). Teaching, learning, and using spectroscopy with commercial, off-the-shelf technology. *Applied Spectroscopy*, **64**(9), 256A.

[3] Asep Nandiyanto, Rena Zaen, Rosi Oktiani, Ade Gafar Abdullah and Lala Riza (2018). A simple, rapid analysis, portable, low-cost, and Arduino-based spectrophotometer with white LED as a light source for analyzing solution concentration. *Telkomnika (Telecommunication Computing Electronics and Control)*, **16**, 580-585.

[4] Daniel R. Albert, Michael A. Todt, and H. Floyd Davis (2012). A low-cost quantitative absorption spectrophotometer, *Journal of Chemical Education*, **89**(11), 1432–1435.

[5] K. Knagge and D. Raftery (2002). Construction and evaluation of a LEGO spectrophotometer for student use, *The Chemical Educator*, **7**(6), 371–375.

[6] Anis Yuniati, Rochan Rifai (2019). Study of simple spectrophotometer design using LDR sensors based on arduino uno microcontroller. *Journal of Physics: Conference Series*, 1153.

[7] V.R. Pereira and B.S. Hosker (2019). Low-cost (<€5), open-source, potential alternative to commercial spectrophotometers. *PLoS Biology*, **17**(6).

[8] Elise K. Grasse, Morgan H. Torcasio, and Adam W. Smith (2016). Teaching UV–Vis spectroscopy with a 3D-printable smartphone spectrophotometer. *Journal of Chemical Education* **93**(1), 146-151.

[9] Kevin Murphy, Brendan Heery, Timothy Sullivan, Dian Zhang, Lizandra Paludetti, Noel O'Connor, Dermot Diamond and Fiona Regan (2014). A low-cost autonomous optical sensor for water quality monitoring. *Talanta*, **132**, 520-527.

[10] Alexandro Fonseca and Ivo Raimundo Jr (2004). A multichannel photometer based on an array of light emitting diodes for use in multivariate calibration. *Analytica Chimica Acta*, **522**, 223-229.

[11] A.F. Fonseca and I.M. Raimundo (2007). A simple method for water discrimination based on a light emitting diode (LED) photometer. *Analytica Chimica Acta*, **596**(1), 66-72.

[12] Germano Veras, Edvan Silva, Wellington Lyra, Sófacles Soares, Thiago Guerreiro and Sérgio Santos. (2009). A portable, inexpensive and microcontrolled spectrophotometer based on white LED as light source and CD media as diffraction grid. *Talanta*, **77**(3), 1155-1159.

[13] Alejandro Lapresta-Fernández, and Luis Fermin Capitan-Vallvey. (2011). Multi-ion detection by one-shot optical sensors using a colour digital photographic camera. *The Analyst*, **136**, 3917-26.

[14] Yasutada Shimazaki, Shunjiro Watanabe, Minori Takahashi and Masaaki Iwatsuki (2000). A portable spectrophotometer using a white-color light-emitting diode and a charge-coupled device and its application to on-site determination of iron. *Analytical Sciences*, **16**(10), 1091-1093

[15] E. Murray, P. Roche, K. Harrington, M. McCaul, B. Moore, A. Morrin, D. Diamond and B. Paull (2019). Low cost 235 nm ultra-violet light-emitting diode-based absorbance detector for application in a portable ion chromatography system for nitrite and nitrate monitoring. *Journal of chromatography A*, **1603**, 8-14.

[16] Jan Höper (2020). Has the time come to use near-infrared spectroscopy in your science classroom? Using mobile near-infrared spectrometers in case-based health and safety education. *Social Science Review*, **376**, 60.

[17]Mizaikoff B. (2003). Infrared optical sensors for water quality monitoring. *Water Science and Technology*, **47**(2), 35-42.

[18] Iftak Hussain, Kamal Ahamad and Pabitra Nath (2016). Low-cost, robust, and field portable smartphone platform photometric sensor for fluoride level detection in drinking water. *Analytical Chemistry*, **89** (1), 767-775.

[19] M.W. Prairie, S.H. Frisbie, K.K. Rao, A.H. Saksri, S. Parbat and E.J. Mitchell (2020). An accurate, precise, and affordable light emitting diode spectrophotometer for drinking water and other testing with limited resources. *PloS One*, **15**(1), e0226761.

[20] D. González-Morales, A. Valencia, A. Díaz-Nuñez, M. Fuentes-Estrada, O. López-Santos and O. García-Beltrán (2020). Development of a low-cost UV-Vis spectrophotometer and its application for the detection of mercuric ions assisted by chemosensors. *Sensors*, **20**(3), 906.

[21] J. Ma, B. Yang and R.H. Byrne (2012). Determination of nanomolar chromate in drinking water with solid phase extraction and a portable spectrophotometer. *Journal of Hazardous Materials*, **219-220**, 247–252.

[22] A.J. Palma, J.M. Ortigosa, A. Lapresta-Fernández, M.D. Fernández-Ramos, M.A. Carvajal and L.F. Capitán-Vallvey (2008). Portable light-emitting diode-based photometer with one-shot optochemical sensors for measurement in the field. *The Review of Scientific Instruments*, **79**(10), 103105.

[23] M. Sargazi and M. Kaykhaii (2020). Application of a smartphone based spectrophotometer for rapid in-field determination of nitrite and chlorine in environmental water samples. *Spectrochimica Acta Part A: Molecular and Biomolecular Spectroscopy*, **227**, 117672.

[24] D. Santra, S. Mandal, A. Santra and U.K. Ghorai (2018). Cost-effective, wireless, portable device for estimation of hexavalent chromium, fluoride, and iron in drinking water. *Analytical Chemistry*, **90**(21), 12815–12823.

[25] S. Levin, S. Krishnan, S. Rajkumar, N. Halery and P. Balkunde (2016). Monitoring of fluoride in water samples using a smartphone. *The Science of the Total Environment*, **551-552**, 101–107.

[26] M. O'Toole, K.T. Lau, R. Shepherd, C. Slater and D. Diamond (2007). Determination of phosphate using a highly sensitive paired emitter-detector diode photometric flow detector. *Analytica Chimica Acta*, **597**(2), 290–294

[27] Anshuman Das, Akshat Wahi, Ishan Kothari and Ramesh Raskar (2016). Ultra-portable, wireless smartphone spectrometer for rapid, non-destructive testing of fruit ripeness. *Scientific Reports*, **6**, 32504.

[28] Yi Wang, Xiaohu Liu, Peng Chen, Nhung Tran, Jinling Zhang, Wei Chia, Souhir Boujday and Bo Liedberg (2016). Smartphone spectrometer for colorimetric biosensing. *Analyst*, **141**, 3233-3238

[29] Webpage of SparkFun Triad Spectroscopy Sensor – AS7265x (https://www.sparkfun.com/products/15050).

[30] S.W. Hobbs, David Paull and Jonathan Clarke (2017). Marsobot – design and performance characterization of a low-cost, ground-based multispectral camera on an open source rover. *International Journal of Remote Sensing*, **38**, 3635-3655.

[31] S.W. Hobbs, D.J. Paull and T. McDougall (2019). Evaluating low-cost spectrometer designs for utility in reflectance and transmittance applications, *International Journal of Remote Sensing*, **40**(2), 642-669.

[32] Wikipedia page on Arduino Uno (https://en.wikipedia.org/wiki/Arduino_Uno).

[33] Webpage of Arduino (https://www.arduino.cc/).

[34] Github Arduino library for pH sensor (https://github.com/DFRobot/DFRobot_PH).

[35] Github Arduino library for spectral triad (https://github.com/sparkfun/SparkFun_AS7265x_Arduino_Library).

[36] Marco Zennaro, Athanasios Floros, Gokhan Dogan, Tao Sun, Zhichao Cao, Chen Huang, Manzoor Bahader, Hervé Ntareme and Antoine Bagula (2009). On the design of a water quality wireless sensor network (WQWSN) – An application to water quality monitoring in Malawi. *Proceedings of the International Conference on Parallel Processing Workshops*, 330-336.

[37] M.K. Amruta and Satish Turkane (2013). Solar powered water quality monitoring system using wireless sensor network. *International Mutli-Conference on Automation, Computing, Communication, Control and Compressed Sensing (iMac4s), Kottayam*, 281-285.

[38] K.A. Unnikrishna Menon, Divya Pullarkatt and Maneesha Vinodini Ramesh (2012). Wireless sensor network for river water quality monitoring in India. *Third International Conference on Computing Communication & Networking Technologies (ICCCNT), Coimbatore*, 1-7.

[39] Niqin Jing (2018) Application of wireless sensor network in urban intelligent traffic information acquisition. *Automatic Control and Computer Sciences*, **52**(5), 431-438.

[40] Anthony Faustine, Aloys Mvuma, Hector Mongi, Maria Gabriel, Albino Tenge and Kucel Samuel Baker (2014). Wireless sensor networks for water quality monitoring and control within Lake Victoria Basin – Prototype development. *Wireless Sensor Network*, **6**, 281-290.

[41] Howard B. Glasgow, JoAnn M. Burkholder, Robert E. Reed, Alan J. Lewitus and Joseph E. Kleinman (2004). Real-time remote monitoring of water quality – a review of current applications, and advancements in sensor, telemetry, and computing technologies. *Journal of Experimental Marine Biology and Ecology*, **300**(1-2), 409-448.

[42] Jane K. Hart and Kirk Martinez (2006). Environmental Sensor Networks – A revolution in the earth system science? *Earth-Science Reviews*, 78, 177-191.

[43] C.J. Barrow (2012). Biochar – potential for countering land degradation and for improving agriculture. *Applied Geography*, **34**, 21-28.

[44] X. Liu, Z. Li, Y. Zhang, R. Feng and I.B. Mahmood (2014). Characterization of human manure-derived biochar and energy-balance analysis of slow pyrolysis process. *Waste Management*, **34**(9), 1619-1626.

[45] Rashid Miandad, Rajeev Kumar, Mohamed Barakat, Chanbasha Basheer, Asad Aburizaiza, Abdul-Sattar Nizami and Mohammad Rehan (2018). Untapped conversion of plastic waste char into carbon-metal LDOs for the adsorption of Congo red. *Journal of Colloid and Interface Science*, **511**, 402-410.

[46] M. Ahmad, S.S. Lee, X. Dou, D. Mohan, J.K. Sung, J.E. Yang and Y.S. Ok (2012). Effects of pyrolysis temperature on soybean stover- and peanut shell-derived biochar properties and TCE adsorption in water. *Bioresource Technology*, **118**, 536–544.

[47] Dinesh Mohan, Kunwar Singh, Sarita Sinha and Deblina Gosh (2004). Removal of pyridine from aqueous solution using low cost activated carbons derived from agricultural waste materials. *Carbon*, **42**(12-13), 2409-2421.

[48] X. Xu, Y. Zhao, J. Sima, L. Zhao, O. Mašek and X. Cao (2017). Indispensable role of biochar-inherent mineral constituents in its environmental applications – A review. *Bioresource Technology*, **241**, 887–899.

[49] N. Hagemann, K. Spokas, H.-P. Schmidt, R. Kägi, M.A. Böhler and T.D. Bucheli (2018). Activated carbon, biochar and charcoal – Linkages and synergies across pyrogenic carbon's ABCs. *Water*, **10**(2), 182.

[50] Mahtab Ahmad, Anushka Rajapaksha, Jung Eun Lim, Mingwang Zhang, & Nanthi Bolan, Dinesh Mohan, Meththika Vithanage, Sang Soo Lee and Yong Sik Ok (2013). Biochar as a sorbent for contaminant management in soil and water – A review. *Chemosphere*, **99**, 19-33.

[51] Kunwar Singh, Dinesh Mohan, Sarita Sinha, G. Tondon and Deblina Gosh (2003). Color removal from wastewater using low-cost activated carbon derived from agricultural waste material. *Industrial & Engineering Chemistry Research*, 42(9).

[52] D. Mohan, S. Rajput, V.K. Singh, P.H. Steele and C.U. Pittman, Jr (2011). Modeling and evaluation of chromium remediation from water using low cost bio-char, a green adsorbent. *Journal of Hazardous Materials*, **188**(1-3), 319–333.

[53] Arumugam Sivasamy, Kunwar Singh, Dinesh Mohan and M. Maruthamuthu (2001). Studies on Defluoridation of Water by Coal-Based Sorbents. *Journal of Chemical Technology and Biotechnology*, **76**, 717-722.

[54] D. Mohan, A. Sarswat, Y.S. Ok and C.U. Pittman, Jr (2014). Organic and inorganic contaminants removal from water with biochar, a renewable, low cost and sustainable adsorbent--a critical review. *Bioresource Technology*, **160**, 191-202.

[55] Dinesh Mohan, Ankur Sarswat, Vinod Singh, María Alexandre-Franco and Charles Pittman (2011). Development of magnetic activated carbon from almond shells for trinitrophenol removal from water. *Chemical Engineering Journal*, **172**(2-3), 1111-1125.

[56] Stacey Kuznetsov and Eric Paulos (2010). Participatory sensing in public spaces – Activating urban surfaces with sensor probes. *DIS 2010 - Proceedings of the 8th ACM Conference on Designing Interactive Systems*. 21-30.

[57] Quy-Toan Do, Shareen Joshi and Samuel Stolper (2018). Can environmental policy reduce infant mortality? Evidence from the Ganga pollution cases, *Journal of Development Economics*, **133**(C), 306-325.

[58] A. Sukmafitri, A.B.D. Nandiyanto, R. Oktiani, R. Ragadhita and A.G. Abdullah (2019). Temperature on the effectiveness of Arduino-based portable spectrophotometer with white light-emitting diode (LED) as a light source for analysing solution concentration. *Journal of Engineering Science and Technology*, **14**(3), 1653-1661.

[59] V.K. Gupta, Saurabh Sharma, I.S. Yadav and Dinesh Mohan (1998), Utilization of bagasse fly ash generated in the sugar industry for the removal and recovery of phenol and p -nitrophenol from wastewater. *Journal of Chemical Technology & Biotechnology*, **71**, 180-186.

[60] Vinod K. Gupta, Dinesh Mohan, Saurabh Sharma and Kuk T. Park (1998). Removal of chromium (VI) from electroplating industry wastewater using bagasse fly ash – a sugar industry waste material. *The Environmentalist*, **19**, 129-136.

[61] Vinod K. Gupta, Dinesh Mohan and Saurabh Sharma (1998). Removal of lead from wastewater using bagasse fly ash – A sugar industry waste material, *Separation Science and Technology*, **33**(9), 1331-1343.

[62] D. Mohan, D. and K.P. Singh (2002). Single- and multi-component adsorption of cadmium and zinc using activated carbon derived from bagasse – an agricultural waste. *Water research*, **36**(9), 2304-2318.

[63] V. Subramanian, R. van Grieken and L. Van't Dack (1987). Heavy metals distribution in the sediments of Ganges and Brahmaputra rivers. *Environmental Geology & Water Sciences*, **9**, 93-103.

[64] M. Singh, G. Müller and I.B. Singh (2002). Heavy metals in freshly deposited stream sediments of rivers associated with urbanisation of the Ganga Plain, India. *Water, Air, & Soil Pollution*, **141**, 35-54.

[65] Sanjay Dwivedi, Seema Mishra and Rudra Tripathi (2018). Ganga water pollution – A potential health threat to inhabitants of Ganga basin. *Environment International*, **117**, 327-338.

[66] P.C. Abhilash and N. Singh (2009). Pesticide use and application – An Indian scenario. *Journal of Hazardous Materials*, **165**(1-3), 1-12.

[67] Dipak Paul (2017). Research on heavy metal pollution of river Ganga – A review. *Annals of Agrarian Science*, 15, 278-286.

[68] Olga V. Voitkevich, Gennady J. Kabo, Andrey V. Blokhin, Yauheni U. Paulechka, and Margarita V. Shishonok (2012). Thermodynamic properties of plant biomass components – Heat capacity, combustion energy, and gasification equilibria of cellulose, *Journal of Chemical & Engineering Data* **57** (7), 1903-1909.

[69] Webpage of Robu: https://robu.in/

Determination of optimum PH for removal of Congo Red dye from water using energy cane biochar (produced at 600°c) was carried out. Dosage of the biochar was 1000PPM. Removal experiments were done at dye concentration of 25 ppm.

The calibration curves for Congo Red solutions at various PHs are given in Chart 6.

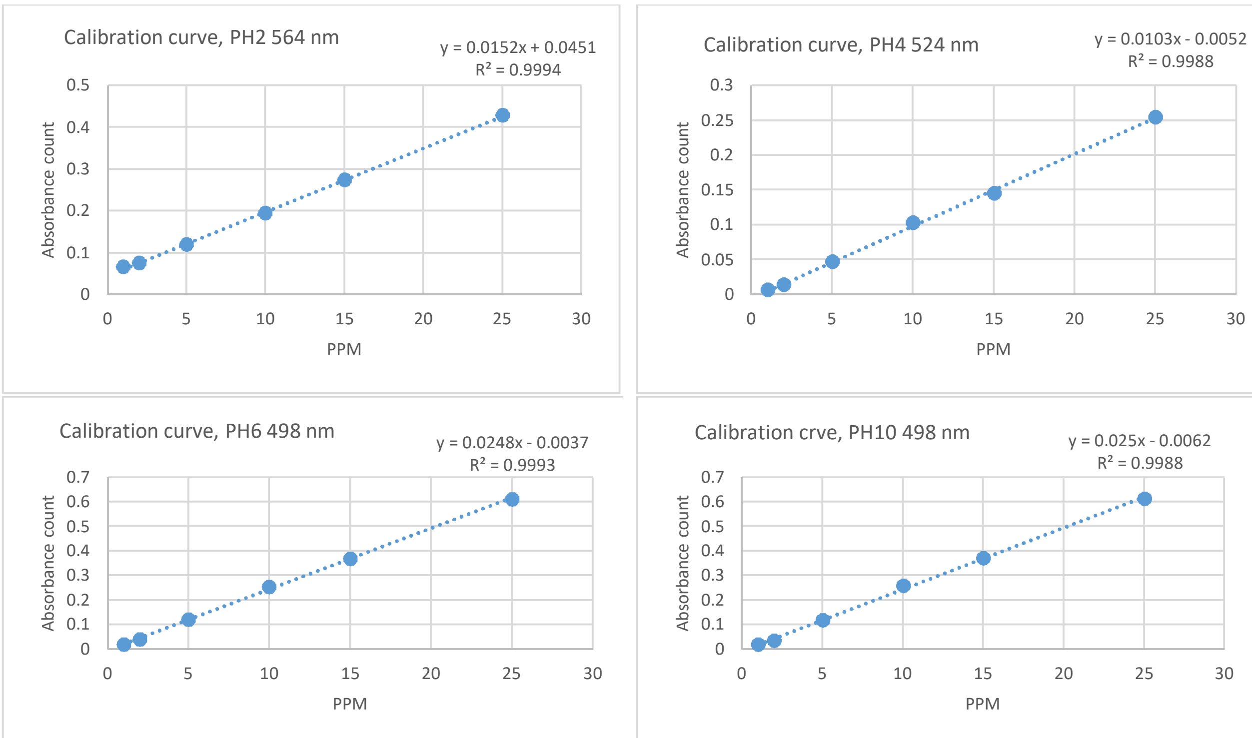

Chart 18: calibration curves at various PHs of congo red solutions

The best removal of Congo Red by energy cane bagasse produced at 600°c is achieved at PH 2 (97.234%). Removal of dye as a function of PH is given in chart 19.

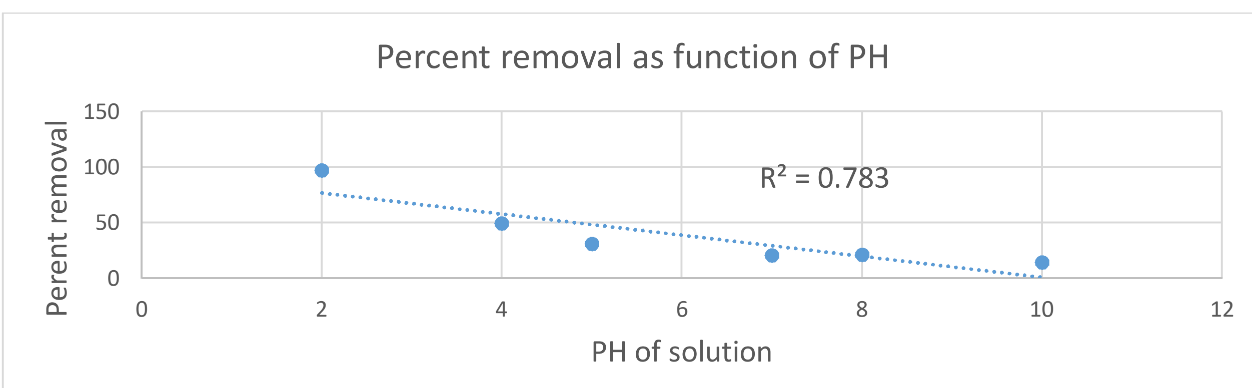

Chart 19: Percent removal as function of PH